

A Novel Four-Point Bend Test for Strength Measurement of Optical Fibers and Thin Beams—Part I: Bending Analysis

Gregory J. Nelson, M. John Matthewson, and Bochien Lin

Abstract—A novel four-point bend apparatus is described for strength measurement of thin compliant beams that avoids the loading and gripping problems associated with other techniques. The apparatus has proved particularly useful for strength measurement of relatively weak optical fibers. In this four-point bend system, loading pin displacement rather than applied load is the measured quantity from which failure stress is calculated, avoiding the load based instability at high deflection. A single-ended support design for the loading pins permits the specimens to be conveniently immersed in the test environment and enables several specimens to be tested simultaneously. Nonlinearities in the deflection/stress relationship are analyzed and a correction factor to the linear bending theory is presented. Friction between the specimen and support pins is found to increase local stresses at the pins. In the second part of this work, a statistical analysis is presented that determines the effective tested length in bending and the tension to bending strength ratio. The predictions of the analysis are confirmed by strength measurements on a weak silica fiber.

I. INTRODUCTION

THIS PAPER describes a novel design of a four-point bend apparatus that is suitable for measuring the strength of thin compliant beam specimens. The work was driven by an interest in strength measurement of cylindrical optical fibers. While the work is applied to circular section beams, it is readily adapted to other cross-sectional geometries. Matthewson [1] provides a comprehensive review of mechanical testing techniques for optical fibers but some key points relevant to this work will be discussed here.

The uniform section of an optical fiber presents a problem for mechanical strength testing since it is difficult to grip specimens without perturbing the results. For a test to be valid, the fiber must be gripped in such a way that it is not damaged by gripping and the stresses at the grip must not exceed the stresses along the tested section; the stresses are

not well known in the gripped region and failure there must therefore be avoided.

Fiber is often tested in uniaxial tension. This technique is time consuming (typically only one sample may be tested at a time), requires large and expensive equipment, and presents gripping problems. The fiber may be held in capstan or pneumatic grips, both of which are prone to slippage and can cause damage to coated fiber and always cause damage to uncoated fiber (optical fiber is typically coated with a layer of polymer to protect it from abrasion). In addition, it is difficult to immerse the fiber in test environments since the tensile test machine cannot normally itself be immersed.

Two-point bending, in which the fiber is bent in a "U" shape between two faceplates, provides an alternative to tensile testing. This technique has been described in detail by Matthewson *et al.* [2] and presents several advantages over tension. In two-point bending, gripping problems are eliminated since the fiber is held in grooved faceplates and is under nominally zero stress at the contact points. The test may be computer controlled and highly automated with break detection being accomplished acoustically. The faceplates holding the specimen are easily immersed in a range of test environments such as liquid nitrogen or an aqueous solution. While bending does not replace tension due to a much shorter tested length (tens of microns compared to meters), it provides a convenient complimentary technique.

Two-point bending is less useful for testing relatively weak fiber since it requires the fiber to be loaded in a bent, i.e., stressed, condition. This small stress may be enough to fracture weak fiber. If the fiber is loaded between widely separated plates the loading stress may be small enough, but the apparatus needs to be large, a long length of fiber is required and the maximum attainable stress rate is limited. While strong silica glass is still the dominant material for optical fibers, other materials are being used to make fibers for various applications. However, these materials generally have poor mechanical properties compared to silica. Two-point bend testing is not so useful for such fiber and for this reason a novel design of the well-known four-point bend test technique is described here that is suitable for testing relatively weak fiber specimens. This apparatus has been used to determine the mechanical properties of heavy metal fluoride fibers [3],

Manuscript received June 5, 1995; revised December 1, 1995. This work was supported in part by the Fiber Optic Materials Research Program at Rutgers University and in part by the New Jersey Commission on Science and Technology.

G. J. Nelson is with the Philips Lighting Company, Bath, NY 14810 USA.

M. J. Matthewson and B. Lin are with the Fiber Optics Materials Research Program, the Department of Ceramic Science and Engineering, Rutgers University, Piscataway, NJ 08855 USA.

Publisher Item Identifier S 0733-8724(96)02951-9.

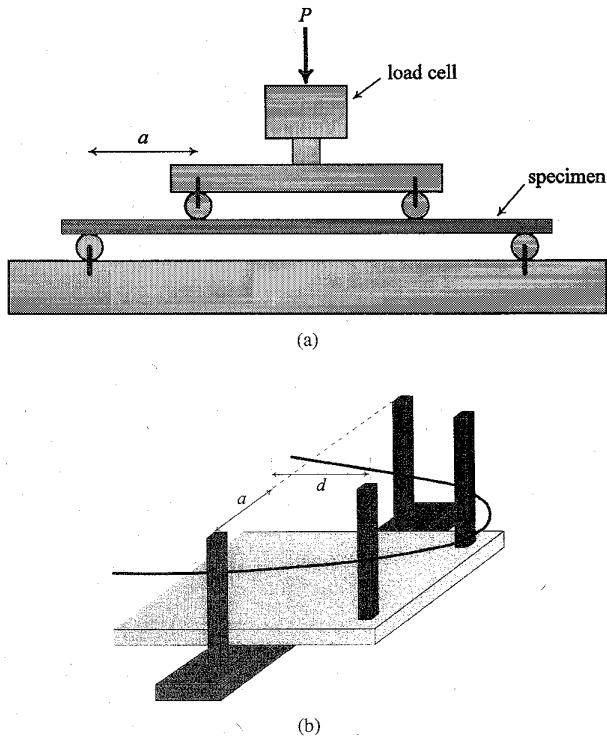


Fig. 1. Schematic of (a) conventional and (b) modified four-point bend apparatus.

[4], [5] (useful for sensor applications and their potential for ultra-low optical loss), chalcogenide fibers (with extended IR transmission), crystalline alumina (sapphire) fibers [6], [7] (useful for laser power delivery and high temperature sensor applications) and silica fibers deliberately weakened by indentation [8].

II. DESCRIPTION OF THE TECHNIQUE

A conventional four-point bend apparatus is shown in Fig. 1(a). In this apparatus the upper (loading) rollers are moved downward against the sample supported by the outer (support) rollers typically at constant velocity by a motor driven screw. The force applied by the loading pins is measured from which the peak stress on the tensile surface of the specimen is calculated.

Fig. 1(b) shows a novel modification of this technique designed for four-point bending of optical fibers. In this system, the two loading pins are mounted on a translation stage movable with respect to the fixed support pins. All the pins are only secured at one end making it simple to load the specimens and submerge both the fiber and pins in a test environment while not immersing the translation stage. The stage is driven by a computer controlled stepper motor. Since the fiber is compliant compared to the support pins, the pins can be assumed rigid. Also, the fiber deflections are large and the applied forces are small; the measured parameter is therefore the movement of the pins, d , which is conveniently given by the distance moved by the stepper motor. The stress

to which the fiber is subjected is then calculated from the displacement, d .

The failure of the fiber may be detected by several techniques but the one found to be most convenient uses acoustic detection. The acoustic emission associated with the fiber fracture is detected by a piezo transducer and trigger circuit which records the displacement at failure. By careful choice of the transducer and its placement, failure of even the weakest fibers, with their correspondingly weak acoustic signature, can be reliably detected. This technique is particularly convenient for use when testing many fibers simultaneously. Provided that the apparatus is constructed with sufficient precision, then several fibers loaded simultaneously will see effectively the same applied stress. Under these circumstances it is not necessary to know *which* specimen breaks, only *when* each break occurs. Acoustic break detection conveniently provides this information.

This four-point bend design offers several advantages and disadvantages compared to other test techniques. All the following points should be carefully considered before selecting this technique.

- i) The fiber is loaded in a straight, i.e., unstressed, shape making it possible, unlike two-point bending, to test very weak fibers without the risk of premature failure. In addition, the fiber is unlikely to be damaged by contact with the loading pins since the inner pins contact the fiber on its compressive surface, while the outer pins contact the tensile surface in a region of low stress. This avoids the gripping problems encountered in tensile testing.
- ii) The single-ended support design for the pins on which the fibers are loaded allows the specimens to be easily immersed in an environment by simply inverting the apparatus over a dish. In this way the strength of fluoride fibers in liquid nitrogen and various aqueous solutions has been measured [3], [5]. However, since bending measures the failure strain, if the failure stress is to be reported, the elastic modulus in the test environment must be known.
- iii) Many samples of the same diameter may be loaded into the apparatus and tested simultaneously by stacking the fibers so they do not touch (20 or more). Acoustic detection may be used to separately record each break. This enables statistically significant results to be obtained rapidly. Also, each specimen experiences exactly the same environment, thus reducing scatter due to fluctuations in the environment, such as the temperature.
- iv) Only a small length of fiber is used for each test (about 50 mm or less). This is an advantage if only limited quantities of fiber are available.
- v) Four-point bend systems that characterize the stress on the fiber by determining the applied load may be limited in their maximum useful deflection. As the deflection increases, the load passes through a maximum (at $d/a \simeq 0.7$) and then decreases. For a dead-weight loading system this represents an instability at which the fiber is catastrophically pulled through the support

pins. No such instability exists for a system which characterizes the fiber stress by the displacement.

- vi) For highly compliant specimens, such as optical fibers and thin beams, the forces required to bend the fiber are small but the resulting deflections are large giving better accuracy for a deflection based system.
- vii) A stepper motor with resolution of $1\ \mu\text{m}$ has been used which gives good accuracy since by a suitable choice of the pin separation, a , it can be arranged that the displacement, d , is a few mm. Absolute accuracy is limited by choosing the point at which the fiber is first subjected to load which is the $d = 0$ position. This may lead to a systematic error in d of typically 5 to $10\ \mu\text{m}$. This error is generally negligible for weak fibers which exhibit considerable scatter in their strength.
- viii) The following analysis for the fiber stress/deflection behavior may be used to calculate a nonlinear stepping profile that results in a linear strain rate during loading.
- ix) Small four point bend fixtures with pins in fixed positions may be inexpensively manufactured for static fatigue testing in virtually any environment. Such fixtures have been successfully used to test heavy metal fluoride fibers under static conditions [5].
- x) The apparatus is inexpensive, compact, and simple to use. Much of the four-point bend apparatus is identical to the two-point apparatus discussed above; namely, the translation stage and stepper motor, the acoustic break detection system and elements of the control software. Therefore, a single system can be used to test in both two- and four-point bending thus covering the complete strength range of interest (from about 0.01% to 20% strain to failure).
- xi) Unlike the stress distribution in tension, the distribution in bending is nonuniform. Therefore, if fibers with a nonuniform flaw distribution are to be tested then careful alignment of the specimens is necessary. For example, fibers containing a single flaw, such as a Vickers indent as described below, must be carefully aligned with the flaw located centrally between the pins and on the surface of maximum tension.

There are, however, some questions associated with this four-point bend test that are addressed in this paper.

- i) Simple linear beam bending theory may not be used to relate the fiber stress to the displacement since the displacement is usually large (the linear theory is only valid for $d \ll a$). The fiber stress is therefore not linearly related to load or displacement.
- ii) When the deflection is large, high friction between the fiber and the pins can significantly affect the stress distribution and can cause the fiber to break at the loading pins. Although frictional effects can be accounted for, an appropriate value for the coefficient of friction is required. The tendency of the fiber to break at the pins invalidates the test since a poorly characterized local stress field due to the contact is superimposed upon the bending stresses at this position.

- iii) Stronger fibers may be pushed through the support pins before breaking. There is therefore a maximum stress attainable in four-point bending which is not present in tension or two-point bending. This maximum, however, does depend on the pin spacing which can be chosen to ensure failure.
- iv) The length of fiber tested is typically a few cm which is shorter than a typical tensile specimen but longer than a two-point bend specimen. Statistical size effects mean that the results of four-point bending cannot be directly compared to the results of other test methods.
- v) The length of fiber used in this test is relatively small and hence the results are not useful for characterizing the strength of long lengths of fiber. However, tensile testing of meter lengths characterizes the severest flaws which are often processing related. The bend test usually explores the properties of the material between the severest flaws and therefore characterizes the tensile strength that can potentially be achieved by better processing. The combination of bending and tensile results is therefore useful for process control applications. This means that this "disadvantage" is advantageous in some cases.

These difficulties are addressed in this paper which presents an analysis for the nonlinear bending, including frictional effects. In the second part of this work the statistical effects are also addressed.

III. ANALYSIS

Although the authors are unaware of any documented use of a deflection based four-point bend apparatus for optical fiber testing, some work has been published on the analysis of the nonlinear load-stress relationship in the more conventional four-point bend apparatus. Vrooman and Ritter [9] present a detailed analysis of a load-based large deflection four-point bend test. Though the analysis was complete in dealing with the nonlinearities of four-point bending, it stopped at the so-called load based instability or "pull through." Ritter and Wilson [10] later considered the effects of friction between the specimen and the loading rollers. Again, a load based system was analyzed and friction was observed to affect the maximum stress before pull through, hence changing the test results. They concluded that the apparatus should be designed by placing the pins so as to avoid the instability and the complexities of analyzing it. Ohtsuki [11] presented both numerical and analytical analyses of four-point bending including the effects of friction and his results are identical to those of the earlier work. Although his analysis was carried to full deflection, it was also load based and he directed his discussion toward the region before the load based instability. It should be noted that his analytical results are not expressible in closed form and require complex numerical analysis to extract useful information. For practical purposes, it is at least as convenient to use a completely numerical approach.

This paper describes four-point bending used as a deflection based system and extends the range of the technique to higher deflections. We present a numerical analysis for the stress

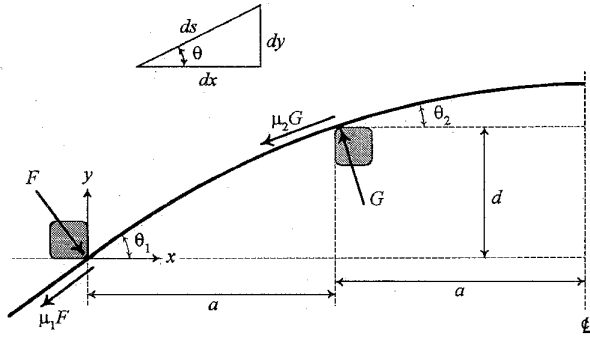


Fig. 2. Schematic of forces imposed on a symmetrical half of the fiber by the support pins.

distribution as a function of the applied deflection. In the second part of this work, the analysis is extended to examine the effect of the statistical nature of fiber strength. In particular, the effective length of fiber under test in bending is determined and the distribution of expected fracture origin positions is examined.

Fig. 2 defines the geometry of half of the bent fiber and the various parameters that will be used in the analysis. It is assumed that the friction is coulombic with coefficients μ_1 and μ_2 acting between the fiber and the outer and inner pins, respectively. The direction of the friction forces are for the sliding direction caused by increasing d . Assuming linear elasticity, the well-known bending equation that describes the profile of the fiber is given by

$$\frac{1}{R} = \frac{M}{EI} = \frac{\frac{d^2 y}{dx^2}}{\left[1 + \left(\frac{dy}{dx}\right)^2\right]^{3/2}} \quad (1)$$

where R is the radius of curvature of the bend, M is the bending moment acting on the fiber, E is the Young's modulus of the fiber, and I the second moment of cross-sectional area ($= \frac{1}{4}\pi r^4$ for a cylindrical specimen of radius r). The maximum strain on the tensile surface of the bent fiber is then simply r/R . In linear bending theory it is assumed that $dy/dx \ll 1$ and it may readily be shown that the maximum strain is then given by

$$\varepsilon = \frac{r}{R} = \frac{3dr}{4a^2}. \quad (2)$$

This strain is uniform between the inner pins $a \leq x \leq 3a$ and decreases linearly to zero at the outer pins, $x = 0$ and $x = 4a$. If the deflection is not small, dy/dx cannot be neglected in (1). To solve (1) in the general case, distinct solutions will be found in the regions $0 \leq x \leq a$ and $a \leq x \leq 2a$. The bending moments in these regions may be related to the reaction forces between the fiber and the pins (Fig. 2)

$$M_1 = F[x(\cos \theta_1 + \mu_1 \sin \theta_1) + y(\sin \theta_1 - \mu_1 \cos \theta_1)], \quad 0 \leq x \leq a \quad (3)$$

$$M_2 = M_1 - G[(x-a)(\cos \theta_2 - \mu_2 \sin \theta_2) + (y-d)(\sin \theta_2 + \mu_2 \cos \theta_2)]. \quad a \leq x \leq 2a. \quad (4)$$

Stability in the y direction gives a relationship between the reactions and angles

$$G = \frac{F(\cos \theta_1 + \mu_1 \sin \theta_1)}{\cos \theta_2 - \mu_2 \sin \theta_2}. \quad (5)$$

As the above differential equation has no closed form solution, a fourth order Runge-Kutta technique was utilized to obtain numerical solutions of (1) using a similar approach to that used by Vrooman and Ritter [9]. For a given starting slope, θ_1 , and a trial value of the reaction, F , (1) is combined with (3) and integrated from $x = 0$ to $x = a$. At this point the reaction, G , is calculated from (5) and the integration proceeds using (1) and (4) until $x = 2a$. In general, dy/dx is not zero at this position, as is required by symmetry; the process is therefore repeated under the control of a secant algorithm using different values of F until a value is obtained for which dy/dx is sensibly zero. This technique then gives the deflection and strain profile along the fiber for a given θ_1 (or more usefully, d/a). Different coefficients of friction can be specified for the support and loading pins to observe frictional effects. Throughout this analysis the fiber radius, r , is considered small compared to a .

In addition to the deflection-based calculations described above, the program has been used to determine fiber stress as a function of pin load for various values of μ . The results are found to be in close agreement with the previous analysis for the load-based system [9], [11]. This verifies the reliability of the computer code.

The support pins most conveniently have a circular section since this shape is easily fabricated and presents a smooth surface where it makes contact with the fiber. The finite size of round pins means that the points of contact between the pins and the fiber move as d increases. This effect has been ignored in our analysis but was included in Vrooman's treatment [9]. Ritter and Wilson [10] later concluded the effect was negligible for pins that are small compared with the length of the specimen (which is usually the case for optical fiber). To remove this as a source of error, a four-point bend apparatus has been constructed using square pins [Fig. 1(b)] whose edges are carefully rounded to a radius of $\sim 200 \mu\text{m}$. This gives an effective pin radius of $\sim 200 \mu\text{m}$ which is insignificant compared to any reasonable value of a , while giving considerable pin stiffness. The pins are positioned so that the inner edges of the outer pins are separated by $4a$, and the outer edges of the inner pins are separated by $2a$, ensuring the correct contact geometry. The small contact area (and high contact stresses) between the fiber and pins has not been observed to cause preferential failure at the pins [8], [7], [5].

All results presented below are expressed in terms of dimensions that have been normalized by dividing by the pin separation, a , so that the results may be applied to any size apparatus. The stress on the fiber additionally depends on the normalized fiber radius r/a and the Young's modulus E . To avoid introducing any extra parametric dependence, the normalized curvature a/R is discussed rather than the stress itself. The stress may then be calculated for a given fiber radius

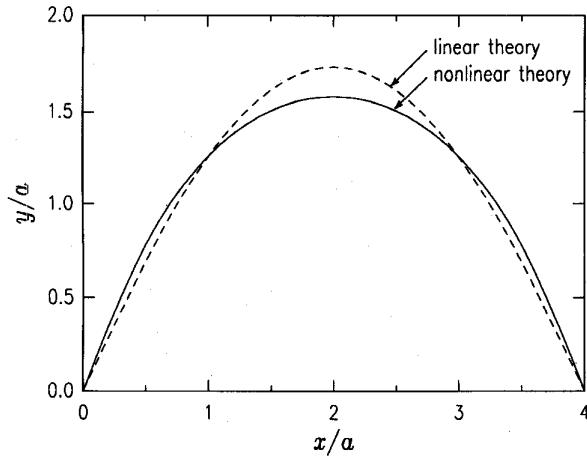


Fig. 3. Comparison of the normalized deflection profile for the linear and nonlinear theories ($d/a = 1.26, \theta_1 = 60^\circ$ and $\mu = 0$).

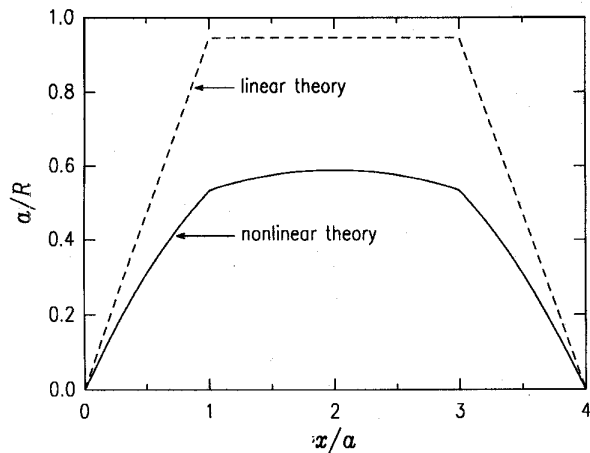


Fig. 4. Comparison of the normalized curvature profile for the linear and nonlinear theories ($d/a = 1.26, \theta_1 = 60^\circ$ and $\mu = 0$).

and pin separation using

$$\sigma = E \frac{r}{R} = E \frac{r}{a} \frac{a}{R}. \quad (6)$$

Fig. 3 shows the profile of the bent fiber for a relatively large deflection $d/a = 1.26 (\theta_1 = 60^\circ)$ for zero friction, $\mu_1 = \mu_2 = 0$. Significant deviations from the linear bending theory are evident at this deflection. Examining the curvature profile, a/R , in Fig. 4 [which is proportional to the fiber stress, (6)], it is clear that the linear theory significantly overestimates curvature and hence stress on the fiber. In addition, the stress distribution along the fiber is not uniform between the inner pins as the linear theory suggests, but rather takes a maximum at the center of the fiber.

Fig. 5 shows the maximum normalized curvature (which occurs at $x = 2a$) for $\mu_1 = \mu_2 = 0$ as a function of d/a . This shows that the linear theory is a good approximation for $d/a \lesssim 0.4$ but overestimates the stress at deflections beyond that. A peak stress is reached for $d/a \simeq 2$ and any deflection beyond that point does not provide increased stress;

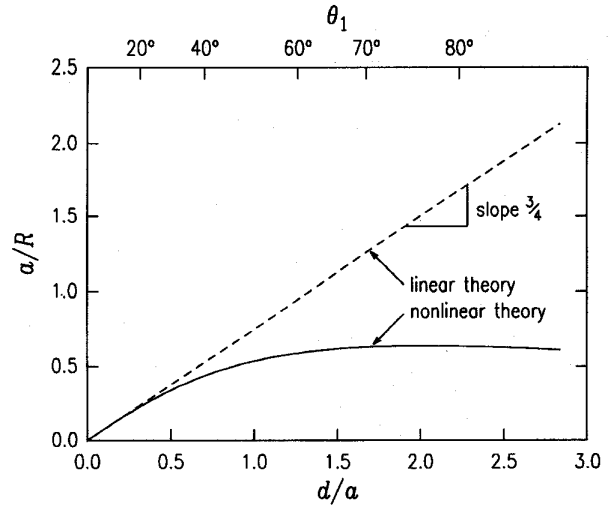


Fig. 5. Comparison of normalized curvature versus normalized pin deflection for the linear and nonlinear theories ($\mu = 0$).

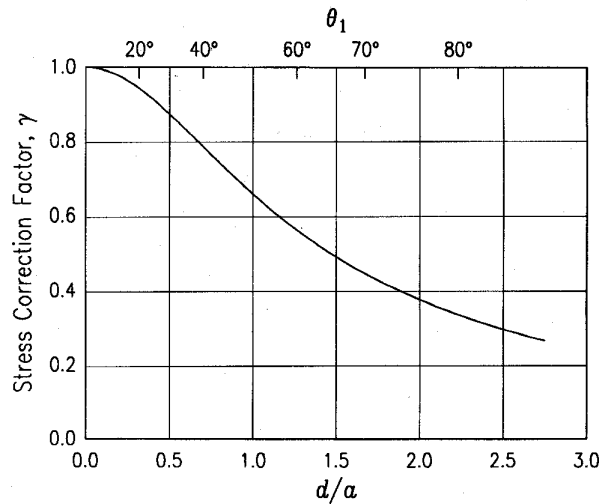


Fig. 6. Correction factor for the linear theory as a function of normalized pin deflection ($\mu = 0$).

this represents the limit of usefulness for the technique. When used in the load-based configuration, the load on the fiber reaches a maximum at $d/a \simeq 0.7 (\theta_1 \simeq 40^\circ)$ [9] which restricts the useful range of the technique.

Fig. 5 may be used to calculate a correction factor, γ , shown in Fig. 6, for the linear bending theory. The stress calculated for a given d/a using the linear theory gives the correct stress when multiplied by this factor. The correction factor is closely approximated by

$$\gamma = 1 - 0.4649\xi^2 + 0.01095\xi^3 - 0.01254\xi^4 \quad (7)$$

where $\xi = \tan^{-1} d/a$, which has a maximum residual error of less than 0.03% in the range $0 < d/a < 2.5$ and is asymptotically correct for small d/a . This empirical form for the factor may be used to calculate the stress on the fiber without detailed analysis of the bend. In particular, the factor

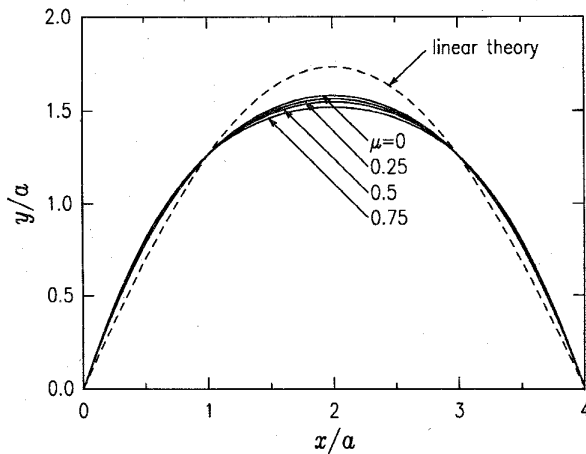


Fig. 7. Normalized deflection profiles for various values for the coefficient of friction between the fiber and the pins ($d/a = 1.26$).

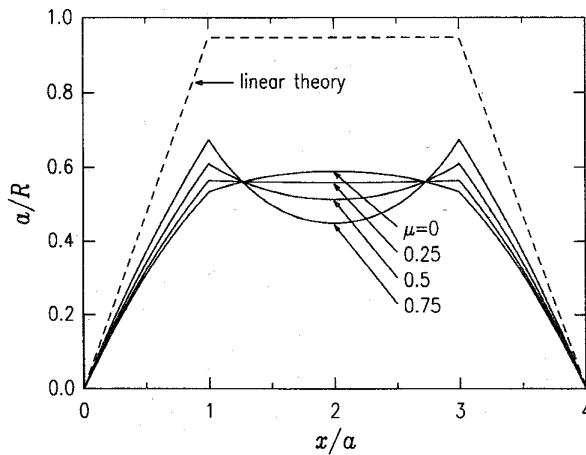


Fig. 8. Normalized curvature profiles for various values for the coefficient of friction between the fiber and the pins ($d/a = 1.26$).

may be incorporated into the computer software controlling the bend apparatus to vary the stepping motor step rate to give, for example, a constant strain rate.

A. Frictional Effects

Figs. 7 and 8 show the effect of friction on the bend profile y/a and normalized curvature a/R (stress), calculated for $d/a = 1.26$ ($\theta_1 = 60^\circ$ when $\mu = 0$). It is assumed that $\mu = \mu_1 = \mu_2$. The friction tends to flatten the fiber profile between the loading pins so that the stress at the middle monotonically decreases with increasing friction. However, the stress at the inner pins monotonically increases with increasing friction. This means that, at this value of d/a , the maximum stress experienced by the fiber first falls with increasing friction but beyond a value of friction of about 0.25, the maximum stress occurs at the inner pins and increases with friction. Therefore, a fiber with a uniform distribution of surface or volume flaws is likely to break at the pins if the friction exceeds 0.25, thus invalidating the test because the unknown contact stress field is superimposed on the bending stress field at this position.

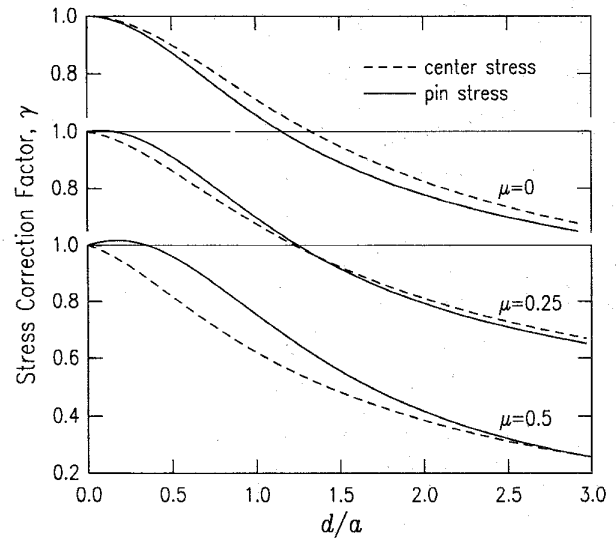


Fig. 9. Correction factors for the stress at the inner support pins (solid lines) and the center of the bend (dashed lines) as a function of d/a for various values of the friction coefficient.

Fig. 9 shows the stress correction factor, γ , (the ratio of the stress predicted by the nonlinear theory to the prediction of the linear theory) as a function of d/a for $\mu = 0, 0.25$, and 0.5 . γ is calculated for the stress both at the loading pins (γ_p) and at the center of the bend, $x = 2a$, (γ_c). For zero friction the stress at the pins is always lower than the stress in the center. At higher friction, the pin stress exceeds the center stress for d/a smaller than some value, substantially so at high friction. The pin stress is always greater than the center stress for nonzero friction and small d/a . The significance of this result to the fracture of specimens with uniformly distributed flaws will be discussed in the second part of this work.

The data of Fig. 9 can be approximated by the following power series which may be used to calculate the pin and center stresses to typically 0.2% precision for $0 \leq d/a \leq 2.5$ and $0 \leq \mu \leq 0.5$

$$\begin{aligned} \gamma_c &= 1 - 0.4455\mu\xi - (0.4557 - 0.3792\mu + 0.5401\mu^2)\xi^2 \\ &\quad - (0.0113 + 0.0048\mu - 0.4210\mu^2)\xi^3 \\ \gamma_p &= 1 + 0.5400\mu\xi - (0.6552 + 0.5968\mu - 0.5893\mu^2)\xi^2 \\ &\quad + (0.1332 + 0.1344\mu - 0.4884\mu^2)\xi^3 \end{aligned} \quad (8)$$

where again $\xi = \tan^{-1}(d/a)$.

In view of the sensitivity of the results to friction, it is desirable to minimize the friction in order to minimize the probability of failure at the loading pins, as well as because it is difficult to determine friction coefficients accurately. This might be achieved by lubricating the pins or coating them with a low friction polymer (e.g., PTFE) or even by mounting the pins in roller bearings. The analysis can then be used to account for any residual friction.

B. In Situ Friction Measurement

The coefficient of friction is sensitive to the nature and surface finish of the fiber and pins, the load, and any surface

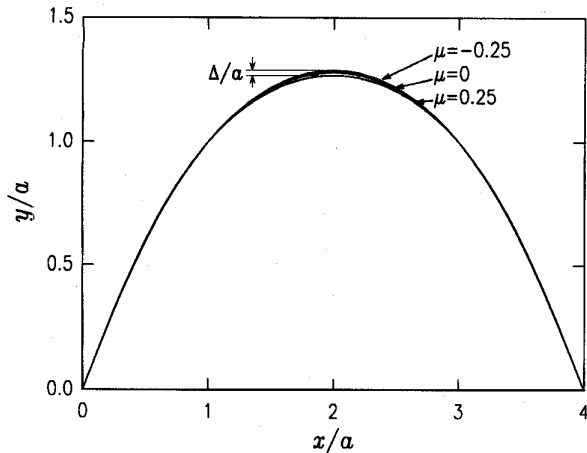


Fig. 10. Normalized deflection profiles for the coefficient of friction, $\mu = 0$ and ± 0.25 showing the position offset, Δ/a ($d/a = 1.26$, $\theta_1 = 60^\circ$).

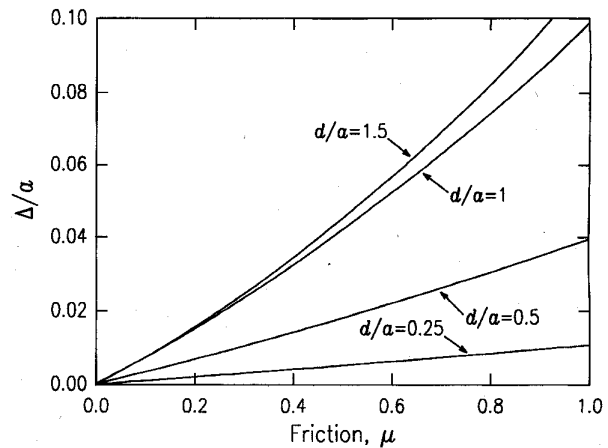


Fig. 11. Normalized position offset, Δ/a , as a function of friction coefficient, μ , for various values of d/a .

contaminants. It is therefore desirable to measure it under identical conditions to the bend test being performed and a technique for doing this has been devised. The fiber is loaded up to a given d/a by increasing d and the position of the center of the fiber is noted. The friction forces are then in the directions shown in Fig. 2. The fiber is then loaded, again to the same d/a , but by **decreasing** d , and the position of the center of the fiber is again noted. The direction of the frictional forces reverses when decreasing d and this can be incorporated into the above analysis simply by using negative values of μ . Fig. 10, for example, shows the fiber profiles for $\mu = 0$ and ± 0.25 for $d/a = 1.26$ (or $\theta_1 = 60^\circ$ when $\mu = 0$, but note, $\theta_1 \neq 60^\circ$ when $\mu \neq 0$). The distance, Δ , between the profiles of positive and negative μ is then a measure of μ . Δ/a is shown as a function of μ for $d/a = 0.25, 0.5, 1.0$, and 1.5 in Fig. 11. The friction can be estimated by interpolation from Fig. 12 after Δ/a is measured. Alternatively, μ can be calculated from the series approximations

$$\begin{aligned} \mu &= 97.51\delta - 510.6\delta^2 & d/a &= 0.25, \\ \mu &= 29.41\delta - 103.9\delta^2 & d/a &= 0.5, \\ \mu &= 13.15\delta - 30.99\delta^2 & d/a &= 1 \end{aligned} \quad (9)$$

where $\delta = \Delta/a$. When μ and d/a are small, Δ is also small and can be difficult to measure. However, under these circumstances the friction has a small effect on the stress. Therefore, the accuracy with which Δ can be measured matches the accuracy to which it needs to be measured.

IV. EXPERIMENTAL RESULTS

The results of the analysis have been verified by direct comparison with a large scale model of a four point apparatus. Pins were set at $d/a = 1.0$ with $a = 250$ mm in a board covered with a large sheet of graph paper. The profile of a fiber supported by the pins was obtained by marking the fiber position on the graph paper. Frictional effects were removed (i.e., $\mu = 0$) by tapping the fiber which causes slip at the pins and removes residual friction forces. The experimental results are compared in Fig. 12 with the predictions of the numerical

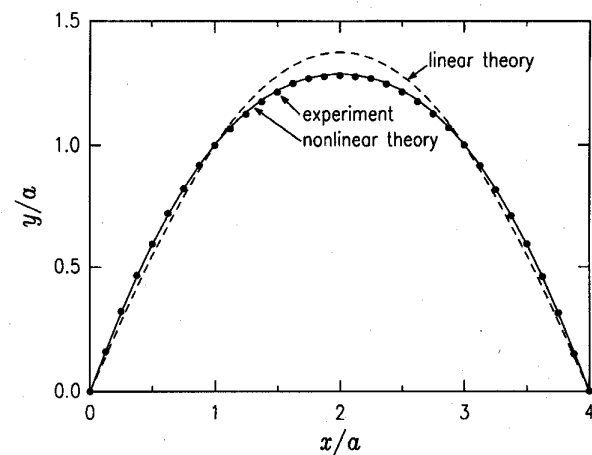


Fig. 12. Comparison of experimental results and predictions of the linear and nonlinear theories for the normalized deflection of the fiber ($d/a = 1.0$).

analysis and the two are indistinguishable from each other within experimental error. They are both significantly different from the prediction of the linear theory which is also shown.

The strength of long lengths of optical fiber is determined by the occasional weak defects that may be separated by meters or km along the length of the fiber. Such defects are difficult to study because they are only detectable after the fiber has failed. Indentation by a Vickers diamond pyramid is commonly used to produce flaws that model practical defects introduced by such processes as abrasion. The technique is particularly convenient because the strength of the indentation defects can be controlled over a wide range by the indentation load. Vickers indentation has provided valuable insight into optical fiber reliability [8], [12]. While a discussion of this topic is beyond the scope of this paper, some of the results we have obtained clearly demonstrate the validity and usefulness of the four-point bending technique.

Fig. 13 shows the strength of indented fused silica fiber as a function of the Vickers indentation load. The measurements were made in a liquid nitrogen test environment. Fused silica exhibits subcritical crack growth; cracks grow slowly under the

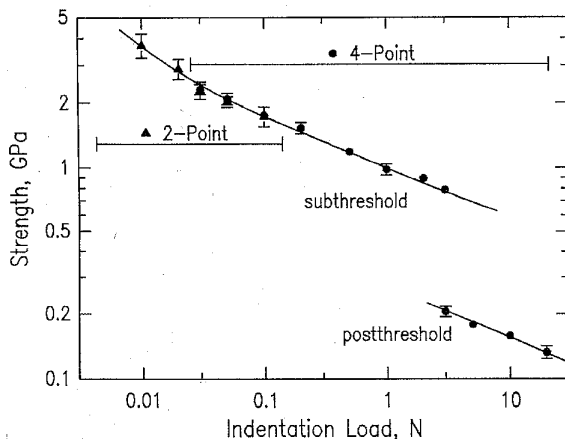


Fig. 13. Liquid nitrogen strength of silica optical fiber as a function of Vickers indentation load for strengths measured in both two- and four-point bending.

combined action of environmental moisture and stresses at the crack tip. The measured strength therefore depends not only on the starting strength of the defect but also on the loading rate and the availability of moisture in the test environment. At liquid nitrogen temperatures the chemical reaction with water is halted and the measured strength is a true estimate of the initial strength of the specimen in the absence of subcritical crack growth. Fig. 13 shows results for both two- and four-point bending. At lower indentation loads the residual strength of the fibers is so high that the fibers are pushed through the inner loading pins of the four-point bend apparatus without failure; in this region two-point bending was employed. At higher loads the residual strength of the fibers is so low that they break while loading them into the two-point bend apparatus so four-point bending was employed here. By using 1000 μm diameter fiber for four-point bending and 100 μm fiber for two-point bending, a region of overlap is formed in which the strength can be measured by either technique and the results for the two techniques are indistinguishable. (In other work we have shown that the mechanical behavior of the fibers used here do not depend on their diameter.) The general trend of the data is independent of the test technique. These results show that the two techniques provide consistent results.

At sufficiently high indentation loads ($\geq 3N$) radial cracks initiate from the indentation site and in this "postthreshold" region the strength is substantially lower than in the "subthreshold" region which leads to the discontinuous strength behavior observed in Fig. 13. These results are qualitatively identical to the earlier work of Dabbs and Lawn [13] and Jakus *et al.* [14] except in two regards. First, their strength measurements under nominally similar indentation loads are substantially lower due to their "inert" environment being dry nitrogen; residual moisture on the fiber surface and in the environment is sufficient to reduce the strength. Second, our data are much more extensive. The earlier work employed tensile testing for the subthreshold indentation defects. This is limiting because the fibers sustain damage diametrically opposite the indentation site where they are supported during indentation. At low indentation loads this damage is more

severe than the indentation itself leading to preferential failure away from the indent. In contrast, the surface diametrically opposite the indentation is in compression in bending tests and so the damage introduced there during indentation does not perturb the results. While this idea was the principal driving force behind development of the bend apparatus discussed here, the apparatus has been found extremely useful in other contexts.

The four-point bending results shown in Fig. 13 were calculated after correction for both nonlinear bending and fiber/pin friction. Measurements of Δ for 100 μm diameter fiber for $d/a = 1$ and $a = 7882 \mu\text{m}$ gave $\Delta/a = 0.0023$; (9) then gives $\mu = 0.03$. The friction has also been estimated by balancing a fiber horizontally on two support pins and then tilting the pins until the fiber slips off. The angle the fiber makes with the horizontal when it slips was found to be $\sim 3^\circ$ giving $\mu \sim 0.05$. For this fiber the friction has a negligible influence on the results given the scatter in the experimental data. The strongest 1000 μm diameter fibers failed at $d/a \sim 0.5$ giving a stress correction factor of $\sim 90\%$. While these results do not provide definitive verification of the nonlinear analysis, which differs little from the linear theory in this region, they do demonstrate the usefulness of the four-point bending technique and consistency with other techniques.

The fiber used in the above experiments had been stripped of its polymer protective coating before indenting and strength testing. The pin/fiber friction was measured for coated fiber and was found to be 0.44; the much higher value results from the high compliance of the coating giving a large contact area with the loading pins. Fig. 9 shows that, except for small and large values of d/a , the pin stress is substantially higher than the stress at the center of the bend. Therefore, coated fiber with flaws uniformly distributed in their surface or volume should be tested at small d/a in order to avoid failure at the loading pins due to the statistical effects to be discussed in Part II of this work. However, these statistical considerations are not relevant to the indented fibers discussed above because they contain only a single flaw that is not distributed in position.

V. DISCUSSION AND CONCLUSION

The deflection-based four-point bending technique described here provides an extremely useful and convenient method for strength testing thin beams and relatively weak (compared to pristine silica) optical fibers. The technique has many advantages which include the ability to test many specimens simultaneously. It is also simple to immerse the specimens in a test environment without exposing the apparatus to that environment. The use of a deflection based apparatus allows extension of the useful bending range to high deflections without experiencing instabilities. Indeed, utilizing the nonlinear bending analysis, strains may be accurately calculated for $d/a \lesssim 2$. The analysis has been used to generate numerical correction factors for the linear theory so that the correct stress on the fiber can be conveniently calculated without detailed analysis of the bend. Approximate power series representations of the results are given in order to facilitate such calculations.

The presence of friction between the fiber and support pins causes a shift in the stress distribution and may cause preferential breakage at the pins if the friction coefficient exceeds about 0.25. It is therefore recommended that the friction be reduced to a minimum through the use of low friction pin materials or lubricants. A simple *in situ* technique has been described for measuring the friction so that it can be accounted for when analyzing results.

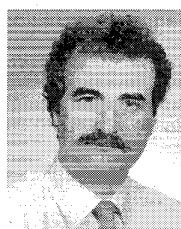
Experimental results show good agreement with the theory presented here. The four-point bending technique has successfully determined the strength of deliberately weakened fibers over a wide range and gives results that are consistent with other techniques. It has enabled us to obtain strength data in a region that is difficult to access using other techniques such as tension or two-point bending.

REFERENCES

- [1] M. J. Matthewson, "Optical fiber mechanical testing techniques," in *Proc. Soc. Photo-Opt. Instrum. Eng. Critical Rev.*, 1994, vol. CR50, pp. 32–59.
- [2] M. J. Matthewson, C. R. Kurkjian, and S. T. Gulati, "Strength measurement of optical fibers by bending," *J. Amer. Ceram. Soc.*, vol. 69, pp. 815–821, 1986.
- [3] J. J. Colaizzi, M. J. Matthewson, T. Iqbal, and M. R. Shahriari, "Mechanical properties of aluminum fluoride glass fibers," in *Proc. Soc. Photo-Opt. Instrum. Eng.*, 1991, vol. 1591, pp. 26–33.
- [4] J. J. Colaizzi, M. J. Matthewson, M. R. Shahriari, and T. Iqbal, "Environmental effects on the mechanical properties of aluminum fluoride glass optical fibers," *Ceram. Trans.*, vol. 28, pp. 579–586, 1992.
- [5] J. J. Colaizzi and M. J. Matthewson, "Mechanical durability of ZBLAN and aluminum fluoride-based optical fiber," *J. Lightwave Technol.*, vol. 12, pp. 1317–1324, 1994.
- [6] G. N. Merberg and J. A. Harrington, "Single-crystal fibers for laser power delivery," in *Proc. Soc. Photo-Opt. Instrum. Eng.*, 1991, vol. 1591, pp. 100–108.
- [7] ———, "Optical and mechanical properties of single-crystal sapphire optical fibers," *Appl. Opt.*, vol. 32, pp. 3201–3209, 1993.
- [8] B. Lin, M. J. Matthewson, and G. J. Nelson, "Indentation experiments on silica optical fibers," in *Proc. Soc. Photo-Opt. Instrum. Eng.*, 1990, vol. 1366, pp. 157–166.
- [9] D. L. Vrooman and J. E. Ritter Jr., "Nonlinear behavior of thin beams in four-point bending," *Bull. Am. Ceram. Soc.*, vol. 49, pp. 789–793, 1970.
- [10] J. E. Ritter, Jr., and W. R. D. Wilson, "Frictional effects in four-point bending," *ASLE Trans.*, vol. 18, pp. 130–134, 1974.
- [11] A. Ohtsuki, "An analysis of large deflections in a four-point bending with friction at all supports," *Bull. J. SME*, vol. 29, pp. 1377–1382, 1986.
- [12] M. J. Matthewson, "Optical fiber reliability models," in *Proc. Soc. Photo-Opt. Instrum. Eng. Critical Rev.*, 1994, vol. CR50, pp. 3–31.
- [13] T. P. Dabbs and B. R. Lawn, "Strength and fatigue properties of optical glass fibers containing microindentation flaws," *J. Amer. Ceram. Soc.*, vol. 68, pp. 563–569, 1985.
- [14] K. Jakus, J. E. Ritter Jr., S. R. Choi, T. J. Lardner, and B. R. Lawn, "Failure of fused silica fibers with subthreshold flaws," *J. Non-Cryst. Solids*, vol. 102, pp. 82–87, 1988.

Gregory J. Nelson received the B.S. degree in ceramic engineering from Rutgers University, Piscataway, NJ, in 1991. His undergraduate research, in the Fiber Optics Materials Research Program, concerned the strength and optical testing of optical fibers. He continued his studies as a National Science Foundation Graduate Fellow in the Department of Physics and Astronomy at Rutgers University where he received the M.S. degree in physics in 1995.

As part of the Rutgers University Laboratory for Surface Modification, his research dealt with surface electronic states of transition metal oxides. He is currently at Philips Lighting Corporation, Bath, NY, developing new high intensity discharge lighting technologies.



M. John Matthewson received the B.A. degree in theoretical physics from Cambridge University in 1975. He received the M.A. and Ph.D. degrees in physics in 1978, also from Cambridge University, for his work at the Cavendish Laboratory on contact mechanics and impact erosion.

He continued his work in these areas as concurrently the Goldsmiths' Junior Research Fellow at Churchill College, Cambridge and as a Science Research Council Postdoctoral Fellow. He spent two years at AT&T Bell Laboratories as a postdoctoral

Member of Technical Staff before moving to the IBM Almaden Research Center, San Jose, CA, in 1986. He has been at Rutgers University since 1989 where he is now an Associate Professor in the Fiber Optic Materials Research Program. His research group is principally concerned with the strength and fatigue of optical materials.

Bochien Lin received the B.A. degree in material science and engineering from Tsing-Hua University, Taiwan in 1981. He received the M.S. degree in ceramics from Rutgers University in 1991 and is currently working towards the Ph.D. degree in the Fiber Optic Materials Research Program in Rutgers University. His thesis is concentrated on the application of Vickers indentation techniques to study the strength and fatigue behavior of silica fibers.

From 1983 to 1988, he was with the China Steel Corporation, Taiwan as a QC and Process Engineer of steel-making.